particle approaches close enough to the target nucleus for nuclear forces to be effective, states of the system resulting from the incorporation of the bombarding particle in the target nucleus are very frequently formed. The composite system is referred to as *the compound nucleus* and when it is formed it must have an excitation energy in excess of the binding energy of the bombarding particle. Consider for example the well-studied reaction in which ^{10}B is bombarded with α-particles and protons are emitted. We represent this reaction by

$$^{10}B + {}^{4}He \rightarrow {}^{13}C + {}^{1}H.$$

The yield of protons as a function of the bombarding energy of the α-particle shows certain peaks. These are interpreted as corresponding to the formation of the compound nucleus, in this case ^{14}N, in an unbound state. The energy of this state must be in excess of the binding energy of an α-particle in ^{14}N. That there is physical reality in regarding the reaction as taking place through this intermediate state is shown by the existence of similar resonances in other reactions, for example $^{12}C + {}^{2}H$, which lead to unbound states of ^{14}N with precisely the same energies. In Figure 64 is gathered the wealth of information from a variety of such reactions and their relationships to the excited states of ^{14}N are shown. The question of the competition between the various possible modes of de-excitation of these unbound states is central to the interpretation of such nuclear reactions as they proceed through a compound nucleus. From a general study of nuclear reactions (see W. M. Gibson, *Nuclear Reactions*, Penguin, 1971) it is clear that there are other types of nuclear reactions, namely *direct reactions*, in which a compound nucleus is not created. In a direct reaction a nucleon or group of nucleons is observed to be emitted without any evidence of an unbound state being involved in the process. The distinction between a direct and a compound nuclear reaction becomes difficult to maintain and largely rests on the time elapsing from the arrival of the bombarding particle to the emission of the products. This time, in the case of a direct interaction, will be of the order of the time taken for a nucleon having a velocity one tenth that of the velocity of light to cross a nucleus, which typically will have a dimension of ten fermis. The transit time is thus a few times 10^{-22} s. In the case of a reaction involving a compound nucleus, the time would be expected to be several orders of magnitude longer than this. Unless this were so the compound nucleus could not be expected to show the properties of a quasistationary state.

10.3 Classical radiation theory

10.3.1

Before turning to the quantum theory of radiative transitions it is useful to review certain aspects of classical radiation theory which give some insight into features with which we shall later be concerned. These are

(a) the rate at which energy is radiated, which will be related to the transition probability of quantum theory,

(b) angular momentum and parity considerations, which will be involved when we come to consider selection rules, and

(c) the damping of the radiating system, which gives rise to finite widths associated with the resonant states.

Classically the nucleus is equivalent to a system of moving point charges and magnetic dipoles. In section 7.5 it was shown that the electrostatic potential arising from the most general stationary charge distribution could be conveniently treated as the superposition of the potentials of charge multipoles. Similar considerations, when applied to the time-dependent electric and magnetic radiation fields, show that these may be treated as the superposition of radiation fields from multipoles which, in the case of radiation, will be either electric or magnetic multipoles which vary with time (A. E. S. Green, *Nuclear Physics*, McGraw-Hill, 1955). We shall later see that, in practical cases, the main contribution to the radiation field comes from the lowest-order multipoles. In the static case there was seen to be a monopole contribution corresponding to an equivalent point charge. As we shall be dealing with nuclei of fixed charge, this term has no time variation and hence the lowest-order multipole with which we are here concerned is the dipole. We shall now consider some properties of the radiation field associated classically with an electric dipole. We recall that the nucleus has no static electric dipole moment (see section 7.6) in the ground state or in an excited state which has a definite parity. However we shall later see that there is a quantity equivalent to a time-varying electric dipole moment involved in the transition between stationary states. This gives rise to radiation analogous to the radiation from a classical oscillating electric dipole.

10.3.2 *Classical electric dipole*

Radiation rate. We consider a charge q having a displacement

$$z = a_0 \sin \omega t,$$

and therefore having an oscillating dipole moment

$$p = p_0 \sin \omega t.$$

The instantaneous rate of radiation of energy per unit solid angle at an angle θ, as in Figure 65, is by classical radiation theory (F. K. Richtmeyer and E. H. Kennard, *Introduction to Modern Physics*, McGraw-Hill, 1954)

$$\frac{q^2 f^2}{4\pi c^3} \sin^2 \theta,$$

where f is the acceleration of the particle, and its velocity is much less than c. Note that there is no radiation emitted parallel to the axis of vibration.

We now write

$$f = -\omega^2 a_0 \sin \omega t,$$

and integrate over all angles to find that Ω, the rate at which energy is lost to the dipole oscillator by virtue of radiation, is given by

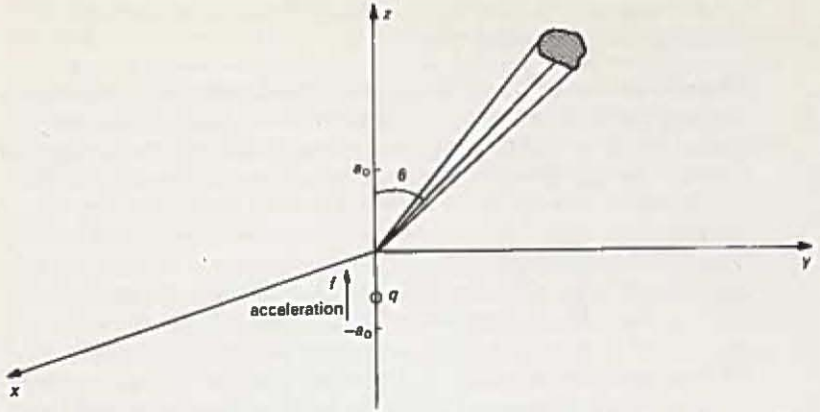

Figure 65 Oscillating dipole consisting of a charge q performing simple harmonic oscillations about the origin along the z-axis

$$\Omega = \frac{2}{3}\frac{q^2}{c^3}\omega^4 a_0^2 \sin^2\omega t.$$

It follows that the energy radiated, per cycle of the oscillation, by the dipole is

$$dW = \frac{2q^2\omega^4 a_0^2}{3c^3}\int_0^{2\pi/\omega} \sin^2\omega t\, dt$$

$$= \frac{2\pi}{3}\frac{p_0^2\omega^3}{c^3}. \qquad 10.1$$

The duration of one cycle is $2\pi/\omega$ and therefore the average rate of radiation is

$$\frac{1}{3}\frac{p_0^2\omega^4}{c^3}.$$

Hence the time taken to radiate an amount of energy equal to that of one quantum, namely, $\hbar\omega$, will be

$$\frac{\hbar 3c^3}{p_0^2\omega^3}.$$

This expression will be the classical analogue of the mean life in the quantum treatment. Consequently the transition probability λ will correspond (see section 2.3) to the reciprocal of this expression, namely

$$\frac{p_0^2}{3\hbar}\left(\frac{\omega}{c}\right)^3.$$

Angular momentum and parity. We noted above that there is no radiation of energy along the z-direction by a dipole lying perpendicular to the xy plane. Retaining the z-axis as the direction of propagation we consider now a radiating system consisting of two electric dipoles, one along the x-axis and one along the y-axis, as in Figure 66, and we suppose there to be a phase difference of $\frac{1}{2}\pi$ between them. This system is equivalent to a single circling charge, the direction of rotation deciding which dipole is leading in phase. At a distant point on the z-axis there will be an oscillating electric field vector E_x parallel to the x-axis associated with the dipole along the x-axis and a similar vector E_y parallel to the y-axis associated with the other dipole. E_x and E_y will, each in synchronism with its parallel dipole, be $\frac{1}{2}\pi$ out of phase and thus give a resultant field vector **E**, which will be of constant amplitude and will rotate with constant angular velocity. Thus the radiation along the z-axis is circularly polarized.

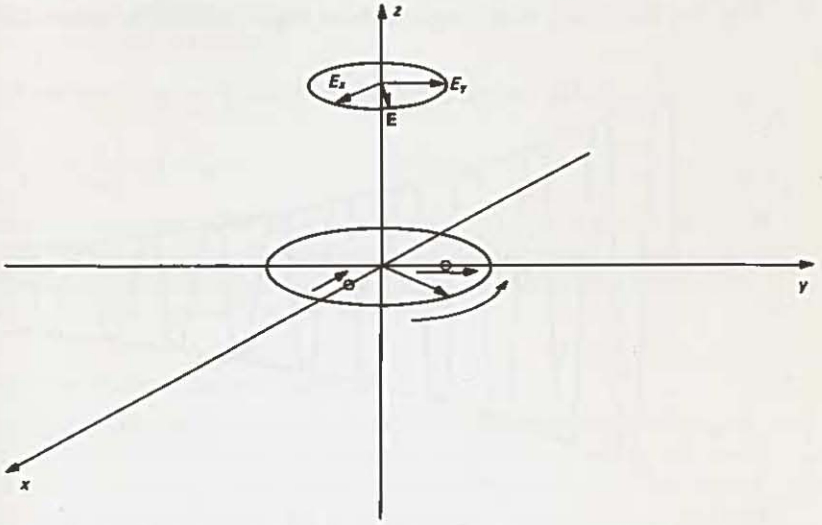

Figure 66 Circularly polarized electric field arising from a charge circulating in the xy plane. The relative phase of **E** and the particle motion will depend on distance along the z-axis

If this radiation were truly transverse (i.e. **E** and **H** perpendicular to each other and to the radius vector) the flow of energy, which is along the direction of the Poynting vector and therefore perpendicular to **E** and **H**, would be radial. However an exact analysis shows that this is not the situation at any finite distance (J. M. Blatt and V. F. Weisskopf, *Theoretical Nuclear Physics*, Wiley, 1963). The Poynting vector is not truly radial. There is thus a 'swirling' of energy about the direction of propagation and associated with this an angular momentum about that direction. This angular momentum will change sign with change in the direction of rotation of the charge and the consequent change in the sense of the circular polarization.

If the parity transformation (substitution of $-x$ for x, $-y$ for y and $-z$ for z) is applied to the system, it amounts to a diametrical displacement of the rotating charge and hence to a change of π in the phase of both equivalent dipoles. It therefore amounts to changing the sign of E and H. There is thus a negative parity associated with this electric dipole radiation.

We note that had we been dealing with a magnetic dipole, which is equivalent to a continuous current rather than a circulating localized charge, the system would not have been altered by the parity transformation. There is thus a positive parity associated with magnetic dipole radiation.

Radiation damping. Reverting to the simple electric dipole of Figure 65, we note that, as a simple harmonic oscillator, it will have an energy content equal to the potential energy when the amplitude is a maximum, i.e. proportional to a_0^2. We now assume that the energy radiated in one period of the oscillation, given by equation 10.1, is very small compared to the total instantaneous energy contained

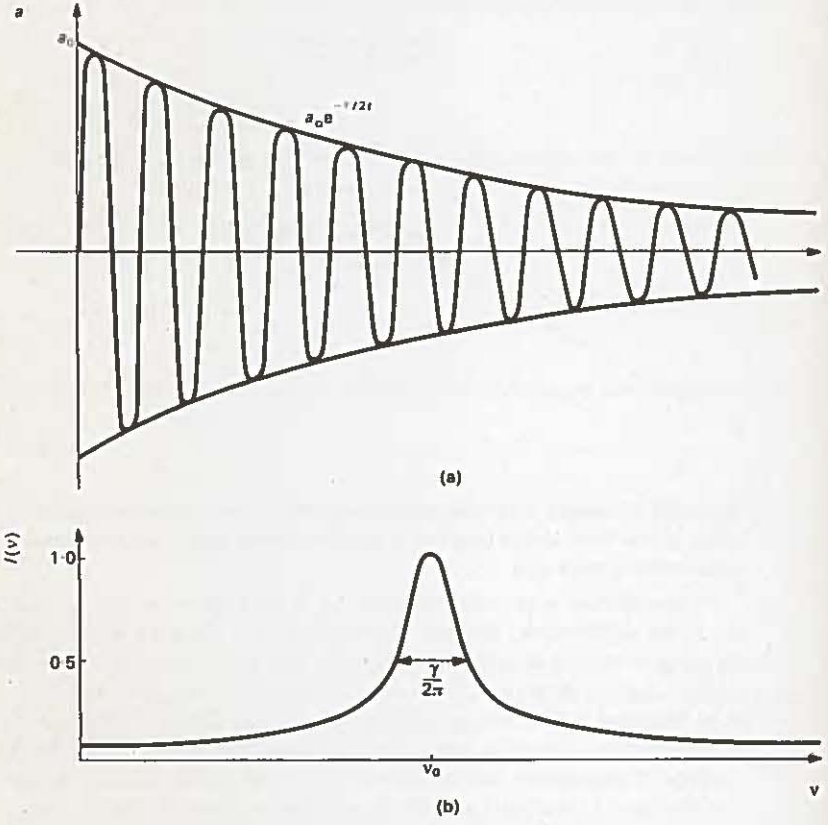

Figure 67 (a) Amplitude variation with time in damped oscillator. (b) Frequency spectrum of damped oscillator

in the oscillator. The energy radiated, being proportional to a_0^2, is thus proportional to the energy stored in the system. Thus the stored energy will decay exponentially with time. If then we write the energy W of the system as

$$W = W_0 e^{-\gamma t},$$

the amplitude of the oscillation will take the form

$$a = a_0 e^{-\gamma/2t}.$$

A plot of the amplitude is shown in Figure 67(a). The technique of Fourier analysis may now be applied to this exponentially decaying function to show that it can be constructed from a superposition of undamped harmonic functions having amplitudes dependent on their frequency and given by the spectral function

$$I(\nu) = \frac{\text{constant}}{(\nu - \nu_0)^2 + \frac{1}{4}(\gamma/2\pi)^2}.$$

This spectral function is illustrated in Figure 67(b). We note that

$$I\left[\nu_0 \pm \frac{\gamma}{4\pi}\right] = \tfrac{1}{2} I(\nu_0),$$

and therefore that the full width at half-maximum of this function is $\gamma/2\pi$. We thus see that, in so far as there is energy radiated, the resonant system is damped and the resonance is no longer infinitely sharp. The half-width is intimately connected with the rate of radiation of energy.

10.4 Quantum theory of radiative transitions

An exact treatment of radiation transitions in terms of quantum mechanics is of a difficulty beyond the scope of this text. It is to be found in an introductory form in R. M. Eisberg, *Fundamentals of Modern Physics*, Wiley, 1961, and in advanced form in J. M. Blatt and V. F. Weisskopf, *Theoretical Nuclear Physics*, Wiley, 1963. We shall here be content to give some of the physical background to the theory and to understand and apply the final results.

The transitions with which we are concerned are spontaneous transitions of an atomic or nuclear system from a state, which we shall characterize by a, to a state of lower energy, characterized by b. These transitions are to be distinguished from *induced* transitions, which are between the same states but stimulated by the presence of an electromagnetic field having a frequency given by $h\nu_{ba} = E_a - E_b$. However, from a consideration of the thermodynamic equilibrium in a closed volume within which a set of atoms or nuclei are emitting and absorbing radiation, the transition rate for spontaneous emission can be related to the transition rate for induced emission and also to the transition rate for absorption. Attention is therefore directed to the problem of the behaviour of the quantum system when it is exposed to an electromagnetic wave, and as a result absorbs or emits energy.

This problem is dealt with by *perturbation theory*. The physical basis of this theory can be described as follows. The wave function of the system in all circumstances can be expressed as a sum of terms according to the equation

$$\Psi = \sum a_n e^{-iE_n t/\hbar} \psi_n.$$

If we assume the system to be in the lower eigenstate b initially, then all the coefficients a_n are zero except a_b and we have

$$\Psi = a_b e^{-iE_b t/\hbar} \psi_b. \qquad 10.2$$

When a perturbing field is applied, the effect is to mix into the wave function a contribution from the wave function of the eigenstate a, so that now we have

$$\Psi = a_b e^{-iE_b t/\hbar} \psi_b + a_a e^{-iE_a t/\hbar} \psi_a. \qquad 10.3$$

Eventually the first term in this expression is reduced to zero and finally we are left with the wave function

$$\Psi = a_a e^{-iE_a t/\hbar} \psi_a \qquad 10.4$$

and the system is then in the eigenstate a.

Now, whereas the time-dependent factor in the product $\Psi^*\Psi$ becomes unity for the wave functions given by equations 10.2 and 10.4, in the case of the function given by 10.3 we have

$$\Psi^*\Psi = a_b^* a_b \psi_b^* \psi_b + a_a^* a_a \psi_a^* \psi_a + a_a^* a_b e^{i(E_a - E_b)t/\hbar} \psi_a^* \psi_b + a_b^* a_a e^{-i(E_a - E_b)t/\hbar} \psi_b^* \psi_a.$$

We note that the product $\Psi^*\Psi$ gives the probability density for the system. When the system is in one or other of its eigenstates we see that the probability density, and hence the charge distribution, is independent of time. When, however, the system is in the state described by equation 10.3, the probability density, and hence the charge distribution, has terms which oscillate with time. We note that the frequency of oscillation of these terms is $(E_a - E_b)/\hbar$, which is precisely the frequency of the photon absorbed or emitted in the transition.

Perturbation theory, as was noted earlier in section 4.9, relates the probability of the transition taking place to the perturbation of the system through *matrix elements*. These matrix elements are constructed from the wave functions of the initial and final states together with an operator which represents the energy arising from the interaction of the quantum system with the perturbing field. The formal definition of the matrix element in the present case will be

$$v_{ab} = \int \psi_a^* V \psi_b \, d\tau,$$

where V is the operator corresponding to the energy of the component charges of the system in the perturbing electric field of the photon.

In the nuclear context we are contemplating photons of energy up to about ten million electronvolts and having wavelengths of 130 fm and upwards. The diameter of a nucleus at the most is about 15 fm. Thus the oscillating electric

field E produced by the photon will, to a first approximation, have a constant value throughout the nuclear volume at any instant. We consider the field E in terms of its components E_x, E_y, E_z. If we choose the centre of the system as the reference point from which potential energy is to be measured, then the electrostatic energy, considering for the present only the x-direction, may be written as

$$V_x = -E_x \sum_r e_r x_r.$$

There will be similar expressions for V_y and V_z. When we now construct the matrix elements according to the formula above, we find occurring integrals of the form

$$\int \psi_a^* \sum_r e_r x_r \psi_b \, d\tau,$$

which from its resemblance to

$$\int \psi_b^* \sum_r e_r x_r \psi_b \, d\tau,$$

the quantum-mechanical analogue of the classical electric dipole moment, we refer to as the matrix element of the x-component of the electric dipole moment, and denote by μ_{xab}. The transition rate for absorption is then found to be

$$\frac{E_x^2}{\hbar^2} (\mu_{xab}^* \mu_{xab} + \mu_{yab}^* \mu_{yab} + \mu_{zab}^* \mu_{zab}),$$

on the assumption that the radiation is not polarized, so that $E_x = E_y = E_z$. When this expression is substituted into the equation relating the spontaneous transition rate S_{ab} to the absorption rate, the dependence on the electric field disappears and it is found that

$$S_{ab} = \frac{32\pi^3 \nu_{ab}^3}{3\hbar c^3} (\mu_{xab}^* \mu_{xab} + \mu_{yab}^* \mu_{yab} + \mu_{zab}^* \mu_{zab}). \qquad 10.5$$

A comparison of equation 10.5 with the expression derived in section 10.3.2 for a classical system shows that the result in the quantum case is in agreement with that for a classical oscillating dipole, whose maximum dipole moment p_0 is given by

$$p_0^2 = 4(\mu_{xab}^* \mu_{xab} + \mu_{yab}^* \mu_{yab} + \mu_{zab}^* \mu_{zab}).$$

10.5 Selection rules for radiative transitions

10.5.1 *Angular momentum (electric dipole)*

The transition probability is seen from equation 10.5 to be finite provided at least one of the dipole matrix elements has a non-zero value. If all the matrix elements are zero, then clearly the transition probability is zero and the transition is said to be forbidden. We now examine the matrix elements to establish the conditions under which they will have non-zero values, and the transition will consequently be allowed.

We are concerned basically with

$$\int \psi_a^* x \psi_b \, d\tau$$

and corresponding integrals involving y and z. To evaluate the integrals requires a knowledge of the wave functions of the two states. We proceed to consider the special case where these wave functions are of the form found in section 6.4 for a single particle in a spherical potential well. The results we shall arrive at are in fact of general validity.

We express the volume integral in spherical coordinates, substitute

$$x = r \sin\theta \cos\phi,$$

represent the wave function as the product $R(r)\Theta(\theta)\Phi(\phi)$ and then have

$$\int_0^\infty R_a^* R_b r^3 \, dr \int_0^\pi \Theta_a^* \Theta_b \sin^2\theta \, d\theta \int_0^{2\pi} \Phi_a^* \Phi_b \cos\phi \, d\phi.$$

Taking the third (or azimuthal) integral and substituting the solution $\Phi(\phi) = Ae^{i(m\phi + B)}$, we have for this integral, apart from constant factors,

$$\int_0^{2\pi} e^{-im_a\phi} e^{im_b\phi} \cos\phi \, d\phi = \tfrac{1}{2} \int_0^{2\pi} [e^{-i(m_a - m_b + 1)\phi} + e^{-i(m_a - m_b - 1)\phi}] d\phi,$$

where m_a and m_b are the magnetic quantum numbers of the two states. Now the expression

$$\int_0^{2\pi} e^{iP\phi} \, d\phi,$$

where P is integral, is zero unless $P = 0$. Hence the azimuthal integral is zero unless $m_a - m_b = \pm 1$, in which case one of the two terms in the above expression will remain finite. By examining the corresponding integral for y it can readily be shown that exactly the same conditions apply.

In the case of the z-coordinate, z is independent of ϕ, and the azimuthal integral reduces to

$$\int_0^{2\pi} e^{-i(m_a - m_b)\phi} \, d\phi.$$

This integral is zero unless $m_a = m_b$.

We arrive at the following conclusion, which is of general validity, namely that the dipole transition may take place only if the difference in magnetic quantum numbers of the two states, Δm, is ± 1 or 0. If $\Delta m = \pm 1$, then $\mu_{zab} = 0$ and, if the transition takes place, the radiation will correspond to that from the classical system of Figure 66. If $\Delta m = 0$, then $\mu_{xab} = \mu_{yab} = 0$ and in this case, if the transition takes place, the radiation will be as for the classical system of Figure 65. We later give further consideration to these two cases.

If, still in terms of the wave functions of a single particle in a potential well, the 'polar' integral

$$\int \Theta_a^* \Theta_b \sin^2\theta \, d\theta,$$

which will involve an orbital quantum number l as well as m for each state, is evaluated, it is found that, in addition to the Δm requirements above, Δl must be ± 1; otherwise the polar integral is zero.

Up to this point we have ignored the intrinsic spin of the single particle. We have to take the spin into account in order to consider the selection rules applicable to the total angular momentum of the particle, j, where $j = l \pm s$. These selection rules are to be found by using a more complete wave function taking into account the spin–orbit interaction. Here we are content to quote the results of such an analysis, namely that for electric dipole transitions $\Delta j = \pm 1$, as for Δl, but that the further possibility of $\Delta j = 0$ also exists. In this latter case Δl is compensated by a change in the spin quantum numbers, a 'spin flip' taking place.

We can now translate the selection rules into terms of the initial and final spin quantum number of two nuclear states. In terms of the single-particle shell model, I, the nuclear spin, is to be equated with j for an odd-A nucleus, and the angular-momentum selection rule for electric dipole radiation becomes $\Delta I = \pm 1$ or 0. The validity of this rule is not limited to states which are describable in terms of the single-particle shell model but is of general validity. Further, it applies also to the states of even-A nuclei, with the proviso that a transition from a state having $I_a = 0$ to a state having $I_b = 0$ (which is a particular case of $\Delta I = 0$) is forbidden. This forbiddenness is understandable since in this case both initial and final states are states of spherical symmetry.

We can represent the angular-momentum selection rules graphically. In Figure 68 the relationships which have to exist between initial- and final-state values of l and m for a single particle are shown for electric dipole transitions.

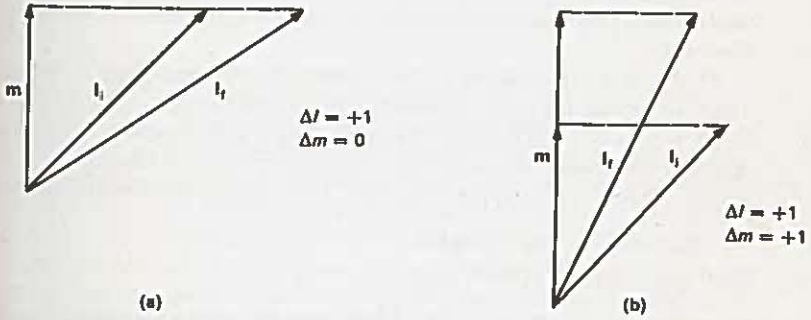

Figure 68 Vector diagram illustrating the selection rules for electric dipole transitions

We can maintain, in considering these diagrams, the picture of a photon having an associated spin 1. In the case of Figure 68(b) we recall that for $\Delta m = \pm 1$, $\mu_{zab} = 0$. We therefore have a situation analogous to the classical case illustrated

in Figure 66. The radiation emitted along the z-axis is circularly polarized and carries angular momentum directed along its direction of propagation. This angular momentum carried by the photon is of course exactly equal to the angular momentum lost by the nuclear system. The radiation emitted in the xy plane is plane polarized and carries angular momentum at right angles to its direction of propagation, i.e. parallel to the z-axis, as before. At oblique angles the polarization is elliptic, i.e. a combination of the two cases discussed above; the associated angular momentum is still parallel to the z-axis. In the case of the situation represented in Figure 68(a), we recall that for $\Delta m = 0$, $\mu_{xab} = \mu_{yab} = 0$ and therefore the corresponding classical situation is that of a dipole oscillating along the z-axis as in Figure 65. In this case there is no emission in the z-direction and the radiation in all other directions is plane polarized with the associated angular momentum lying parallel to the xy plane.

In the case of the nucleus, the diagrams of Figure 68 are still valid if we replace $\mathbf{I}_a$ and $\mathbf{I}_b$ by $\mathbf{I}_a$ and $\mathbf{I}_b$. However in the case of the nucleus there is the additional possibility that $\Delta I = 0$. In this event $\mathbf{I}_a$ and $\mathbf{I}_b$ are to be represented as making equal angles with the z-axis and hence being two generators of a cone with axis Oz such that $\mathbf{I}_a = \mathbf{I}_b + \mathbf{1}$. This vector representation is geometrically possible for all values of I_a and I_b except $I_a = I_b = 0$, which, as we saw above, is not an allowed transition.

10.5.2 *Parity selection rules for electric dipole transitions*

If we apply the parity transformation to the function $\psi_a^* x \psi_b$ we find that there is a change of sign if ψ_a and ψ_b have the same parity and no change of sign if ψ_a and ψ_b have opposite parity. This behaviour arises, of course, from the odd parity of the factor x. It follows therefore that the integration over all space of this function leads to a finite result only if ψ_a and ψ_b have opposite parity. Hence we conclude that for electric dipole transitions a change of parity between initial and final states is a necessary condition for at least one of the matrix elements to be non-zero.

We note that the condition $\Delta l = \pm 1$ ensures that this parity rule is obeyed. This is so because the parity of the wave functions is determined by the sign of $(-1)^l$. We see that this holds for the single-particle wave functions as follows. In spherical coordinates, the parity transformation amounts to substituting $\pi - \theta$ for θ, $\pi + \phi$ for ϕ and leaving r unchanged. These angular transformations lead to

$$\Phi_m(\pi + \phi) = (-1)^{|m|}\, \Phi_m(\phi)$$

and $$\Theta(\pi - \phi) = (-1)^{l+|m|}\, \Theta(\theta).$$

Hence when we take the products of these with the radial wave function we have

$$\psi(r, \pi - \theta, \pi - \phi) = (-1)^l \psi(r, \theta, \phi).$$

It therefore follows that two states differing by one in l-value, as do the states involved in an electric dipole transition, necessarily have opposite parity.

10.5.3 *Selection rules for radiative transitions in the general case*

Many radiative transitions are observed to take place between states whose spins and parities do not satisfy the above selection rules. Only in the case of $I_a = 0 \rightarrow I_b = 0$ is the transition found to be absolutely forbidden. To understand why the transitions still can take place, despite the selection rules not being obeyed, we have to have regard to the assumption made above concerning the nature of the interaction between the nucleus and the electrostatic field. It was assumed that the electrostatic field acted uniformly throughout the nuclear volume. This uniformity is only true to a first approximation and arises from the nuclear dimension being very much smaller than the wavelength of the radiation. It amounts to taking the first term in the series expansion of the harmonic function representing the space dependence of the electromagnetic wave. There will be further terms involving higher powers of x/λ which we neglected. If these terms are included, then the matrix element has to be expressed as a sum of terms of the form

$$\int \psi_a^* x^L \psi_b \, d\tau,$$

where L is now 1, 2, 3, ... The terms in the series get progressively smaller as L increases. However, if, because of a contravention of the selection rules derived above, the term corresponding to $L = 1$ becomes zero, then the transition probability is dominated by the term corresponding to $L = 2$. This integral is termed the electric-quadrupole, or E2, matrix element.

There is the further consideration that no allowance has been made for the interaction of the magnetic field of the wave with the currents and magnetic dipoles involved in the system. Allowance for this interaction introduces magnetic-multipole matrix elements corresponding to magnetic multipole transitions, which we denote by M1, M2, etc.

We consider first the selection rules for E2 transitions. These are arrived at by a consideration of

$$\psi_a^* x^2 \psi_b \, d\tau.$$

Applying the same simple argument as we applied to the electric dipole (i.e. E1) transition above, we see that, since x^2 has positive parity, the initial and final states must be of the same parity, otherwise the E2 matrix element will be zero. The arguments made above with respect to the single-particle wave functions can be repeated for the E2 matrix element and the selection rule arrived at is that $\Delta I = \pm 2, \pm 1$ or 0, with again $I_a = 0 \rightarrow I_b = 0$ being forbidden.

We consider now M1 transitions. We noted above that a magnetic dipole behaves in the opposite manner to an electric dipole under parity transformation. It follows that the parity selection rule for M1 transitions is that the states involved be of similar parity. The angular-momentum selection rules are found in the case of M1 transitions to be the same as for E1 transitions.

In the case of an L-pole transition, the photon can be considered to take away an angular momentum Lh. According to the conservation of angular momentum,

the vectors $\mathbf{I}_a$, $\mathbf{I}_b$ and $\mathbf{L}$ must therefore form the sides of a triangle. This limits the possible values of L, for given I_a and I_b values, to those satisfying the conditions

$$|I_a - I_b| \leq L \leq I_a + I_b.$$

The electric or magnetic character of the transition is determined by the relative parities of the initial and final states, there being no change of parity for electric transitions of even L-values and for magnetic transitions of odd values.

10.6 Transition rates

The transition rate given by equation 10.5 we now see to be valid for E1 transitions only. When we pass to higher multipoles we observed above that we are incorporating additional terms from the expansion of a space factor $\exp(i2\pi x/\lambda)$ in the expression for the field of the electromagnetic wave. As therefore we pass from one multipole order to the next we have to expect an additional factor x/λ to appear in the interaction energy involved in the matrix element. Not only does this introduce the next highest nuclear multipole into our considerations by increasing by one the power of x, but it introduces a factor proportional to $1/\lambda$ (and hence proportional to ν_{ab}/c) into the matrix element. The transition rate, being proportional to the square of the matrix element, in the general case is therefore expected to be proportional to $(\nu_{ab}/c)^{2L+1}$.

A detailed treatment of the general case, given by J. M. Blatt and V. F. Weisskopf, *Theoretical Nuclear Physics*, Wiley, 1963, shows that the result may be written as

$$\lambda = \frac{8\pi(L+1)}{L[(2L+1)!!]^2}\frac{1}{\hbar}\left[\frac{2\pi\nu_{ab}}{c}\right]^{2L+1} B_{ab}(L),$$

where $(2L+1)!!$ represents the product $1 \times 3 \times 5 \times \ldots \times (2L+1)$. When λ, here the transition probability, is written in this way, all of the dependence of the transition rate on the nuclear wave functions is contained in $B_{ab}(L)$, which is termed the *reduced transition probability*. When comparing transition rates for transitions of the same character, for different pairs of states, complications arising from the different transition energies are clearly avoided by comparing the values of $B_{ab}(L)$ rather than comparing the values of the transition probability.

In the case of magnetic transitions, current density plays the role played in electric transitions by charge density. This introducesa factor v/c in the matrix element, and hence a factor $(v/c)^2$ in the transition probability for magnetic transitions as compared to electric transitions, where v is the nucleon velocity and is approximately $\frac{1}{10}c$. The existence of nuclear magnetic moments complicates the issue but does not prevent the magnetic transition rate being significantly smaller than an electric transition of the same multipole order, due allowance having been made for the energy dependence.

The calculation of exact values for transition probabilities requires a detailed knowledge of the nuclear wave functions of the states; usually this is not available. In fact an excellent test of any proposed wave functions is to use them to predict transition rates which may then be compared with measured values. For many purposes, however, it is valuable to compare measured transition rates with those calculated on the basis of the extreme single-particle model. On the assumption of this model, namely that the transition involves a change of state of one nucleon only, Weisskopf (1951) arrived at the following estimates for reduced transition probabilities in the case of electric and magnetic multipoles.

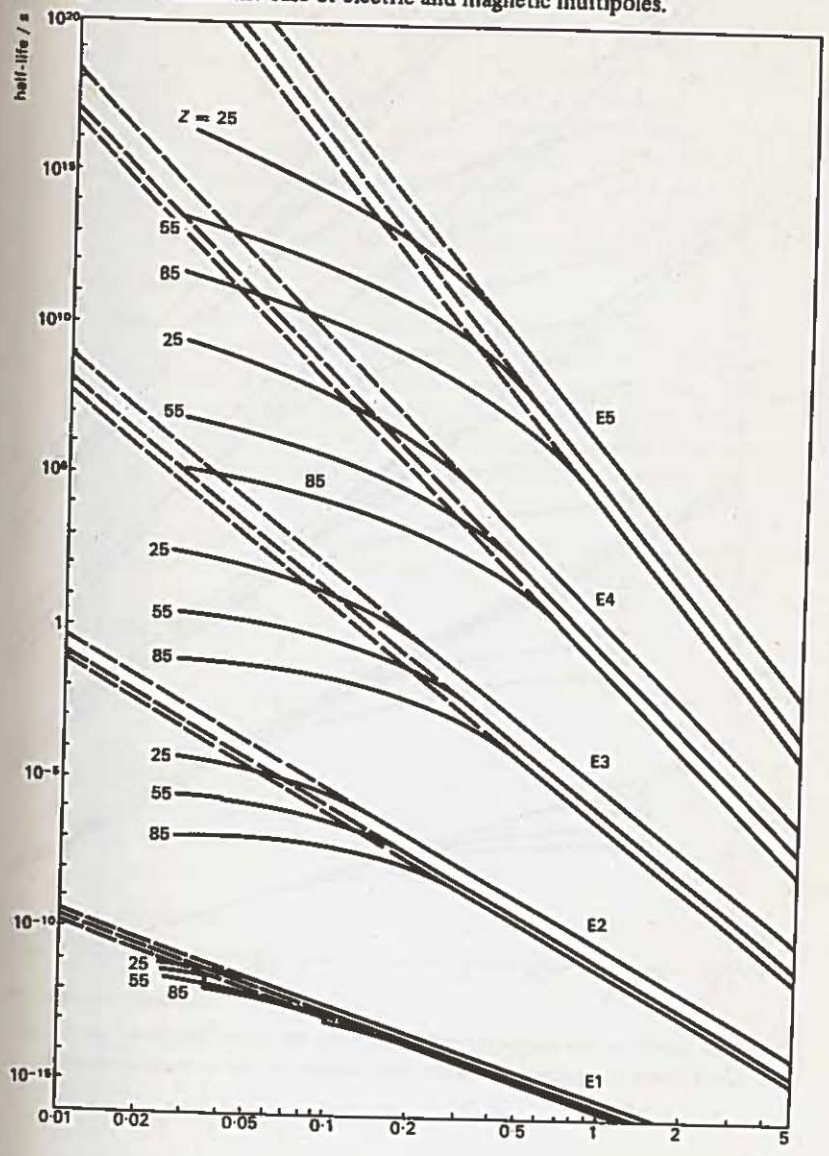

Figure 69 Half-lives for electric multipole γ-ray emission (Weisskopf estimates) with (solid lines) and without (dashed lines) correction for internal conversion

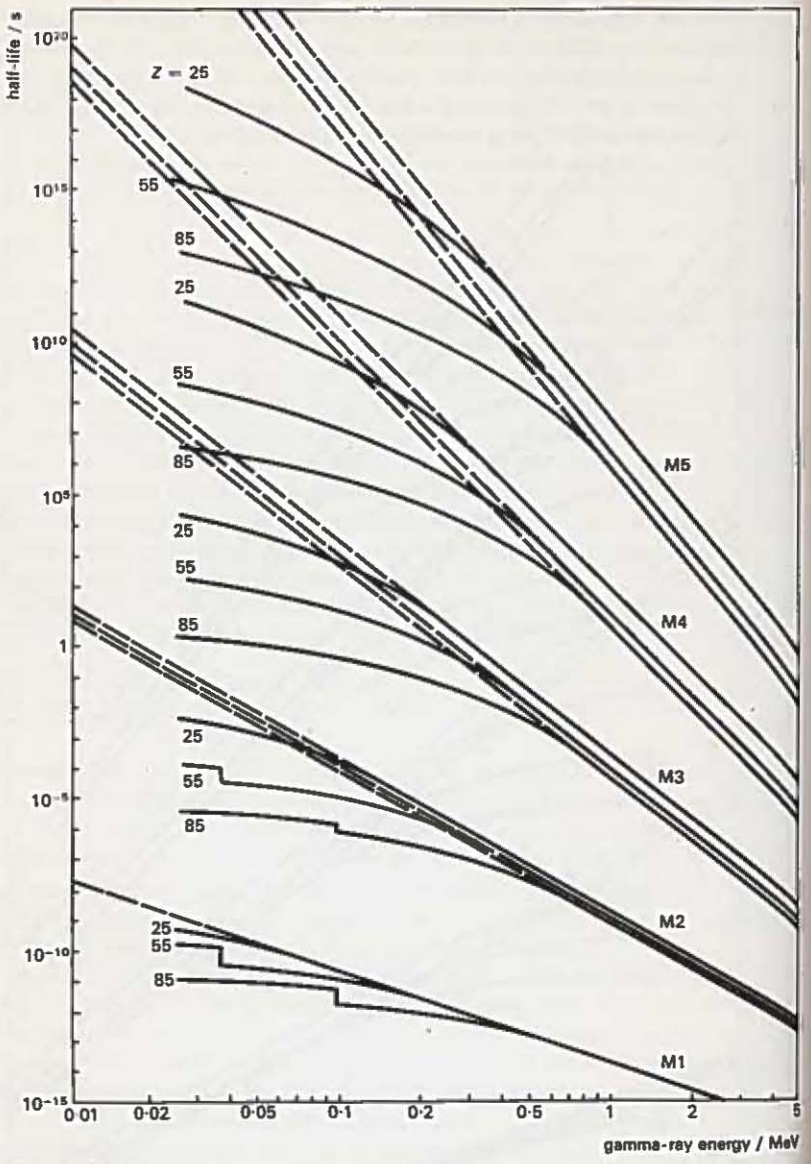

Figure 70 Half-lives for magnetic multipole γ-ray emission (Weisskopf estimates) with (solid lines) and without (dashed lines) correction for internal conversion

$$B(\mathrm{E}L) = \frac{e^2}{4\pi}\left[\frac{3R^L}{L+3}\right]^2,$$

$$B(\mathrm{M}L) = 10\left[\frac{\hbar}{McR}\right]^2 B(\mathrm{E}L),$$

where R is the nuclear radius and M is the proton mass. We may further introduce $R = R_0 A^{\frac{1}{3}}$ and replace the R-dependence by an A-dependence.

These estimates can now be converted into half-life for the excited state. The results of such a conversion are shown in Figures 69 and 70 plotted against the energy of the transition. It is seen that the lowest multipole order permitted by the selection rules is favoured and that electric transitions always proceed faster than magnetic transitions of the same multipole order.

10.7 Level widths

We now consider a transition from an excited state to the ground state, which we assume stable. Just as in the classical theory, as we saw in section 10.3.2, a radiating system is damped and emits a range of frequencies, so in the quantum case we have to assume that the energy level corresponding to an excited state has an energy width which we represent by Γ. We can relate Γ to the mean life τ of the state by Heisenberg's uncertainty principle, which gives

$$\Gamma\tau = \hbar.$$

As in the classical analogue, the energy of the radiation emitted will not, strictly speaking, be monochromatic but will have a spectrum $I(\mathrm{E})$ given by

$$I(\mathrm{E}) = \frac{\text{constant}}{(E-E_0)^2 + \frac{1}{4}\Gamma^2},$$

where $E_0 = E_a - E_b$.

If the final state is not stable but itself has a finite decay probability, then it also will have a level width and Γ will be the sum of the widths of the two levels.

Since $\lambda = 1/\tau$ and $\Gamma\tau = \hbar$, the values of transition probabilities quoted in section 10.6 can be readily translated into level widths. In the case of electric transitions the first few level widths are as follows (E_0 in MeV; $R = 1{\cdot}2 \times A^{\frac{1}{3}}$ fm)

$$(\mathrm{E1}) = 6{\cdot}8 \times 10^{-2} A^{\frac{2}{3}} E_0^3 \text{ eV},$$
$$(\mathrm{E2}) = 4{\cdot}9 \times 10^{-8} A^{\frac{4}{3}} E_0^5 \text{ eV},$$
$$(\mathrm{E3}) = 2{\cdot}3 \times 10^{-14} A^{2} E_0^7 \text{ eV}.$$

In the case of magnetic transitions the results are

$$(\mathrm{M1}) = 2{\cdot}1 \times 10^{-2} E_0^3 \text{ eV},$$
$$(\mathrm{M2}) = 1{\cdot}5 \times 10^{-8} A^{\frac{2}{3}} E_0^5 \text{ eV},$$
$$(\mathrm{M3}) = 6{\cdot}8 \times 10^{-15} A^{\frac{4}{3}} E_0^7 \text{ eV}.$$

The resonances are thus seen to be very sharp, i.e. the energy width of the level is a very small fraction of the γ-ray energy.

10.8 Internal conversion

In the above discussion we have proceeded on the assumption that the system is isolated except for its interaction with the electromagnetic field. This in fact is not strictly correct either for atoms or for nuclei. In normal circumstances atoms are frequently in collision with other atoms and in their collisions energy-transfer processes are involved. As a consequence, there will always be a probability of de-excitation of an excited state by a collision in competition with de-excitation by radiation. Normally this competition is such, in the atomic context, as to suppress all radiative transitions except that of the electric dipole.

Nuclei, on the other hand, are isolated very effectively from each other in ordinary matter by the effect of their screen of orbital electrons. However, in the nuclear case, the very existence of orbital electrons provides a method of de-excitation which competes with radiative transitions. In the neighbourhood of the nucleus the field of the nuclear multipole will act on any electron in that region of space and can communicate the full transition energy to the electron. This energy will usually be much greater than the electron binding energy and consequently the electron will be ejected from the atom. This process is rather misleadingly referred to as *internal conversion*. It must not be thought of as the emission by the nucleus of a photon which is subsequently absorbed by the atomic structure of the same atom. This is a possible process but is much less likely than internal conversion. Internal conversion as a process is distinct from, and competes with, photon emission. The energy is communicated directly to the emitted electron, not by the intervention of an electromagnetic wave.

The competition with radiative transitions is clearly brought out by defining the *conversion coefficient* α as

$$\alpha = \frac{N_e}{N_\gamma},$$

where N_e and N_γ are the experimentally measured numbers of electrons and photons emitted in the same time interval from the same sample. On this definition α can take values from zero to infinity.

The energy of the emitted electron will be given by

$$E_e = E_0 - E_B,$$

where E_0 is the transition energy and E_B the electron-binding energy. In so far as electrons from different shells have finite probability densities close to the nucleus, electrons may be emitted from L, M, . . . shells as well as from the K-shell. These electrons will be experimentally distinguishable because of the difference in E_B. Experimentally we can therefore determine $\alpha_K, \alpha_L, \ldots$, where

$$\alpha_K = \frac{N_K}{N_\gamma}$$

is defined in terms of K-electrons only. It follows from these definitions that $\alpha = \alpha_K + \alpha_L + \alpha_M + \ldots$.

If now we introduce λ_e to represent the probability that an electron be emitted and λ_γ the probability that a photon be emitted we have

$$\alpha = \frac{\lambda_e}{\lambda_\gamma}$$

directly from the definition of α. Internal conversion and radiative transitions are assumed to proceed as independent processes and hence the total transition probability λ is given by

$\lambda = \lambda_e + \lambda_\gamma$.

On this view the lifetime of the state, which is proportional to the reciprocal of λ, will be shortened by the existence of the phenomenon of internal conversion. Support for this view comes from the discovery by Bainbridge and others (1957) that the lifetime of a state in ^{99}Tc was altered by about 0·3 per cent by a change in the chemical composition of the sample. This effect can be entirely accounted for by the difference in the electronic wave functions of the two chemical compounds concerned.

λ_e can be developed, as α was above, in terms of conversion probabilities involving electrons from the different shells, giving $\lambda_e = \lambda_K + \lambda_L + \ldots$.

The calculation of conversion probabilities is in principle straightforward. We start with an initial state consisting of an excited nucleus and a bound electron, and end in a final state with a de-excited nucleus and an electron in a state in the unbound continuum. The transition rate has then to be found from the square of the matrix elements connecting the two states and the density of final states (the so-called *golden rule* which we quoted in section 4.9). The mathematical details are of formidable difficulty even for relatively simple transitions (see E. Segrè, *Nuclei and Particles*, Benjamin, 1964). The results of the mathematical analysis show that the dependence of λ_e on the nuclear multipole moments is exactly the same as the dependence in the case of λ_γ. As a consequence α, the internal conversion coefficient, is independent of the nuclear moments. This has made internal conversion a very important phenomenon in unravelling the character of particular nuclear transitions. α is dependent on the Z-value of the atom involved, as this controls the number of available electrons. α also depends on the transition energy E_0, on the multipolarity of the transitions and on the electric or magnetic character of the transition. These latter factors control the field strength involved in the process.

The Z-dependence of α follows a high positive power (Z^3 in the case of α_K). The E_0 dependence follows a high negative power. As a consequence, internal conversion has its greatest relative importance for high-Z nuclei and low-energy transitions. It is also in these circumstances that the dependence on the character of the multipolarity is greatest. Hence internal conversion has its most significant experimental contribution to make for low-energy transitions in heavy nuclei. Its effectiveness in providing decisive evidence of the character of the transition can be seen from Figure 71, which shows the variation to be expected in the conversion coefficient for transitions of different multipole order.

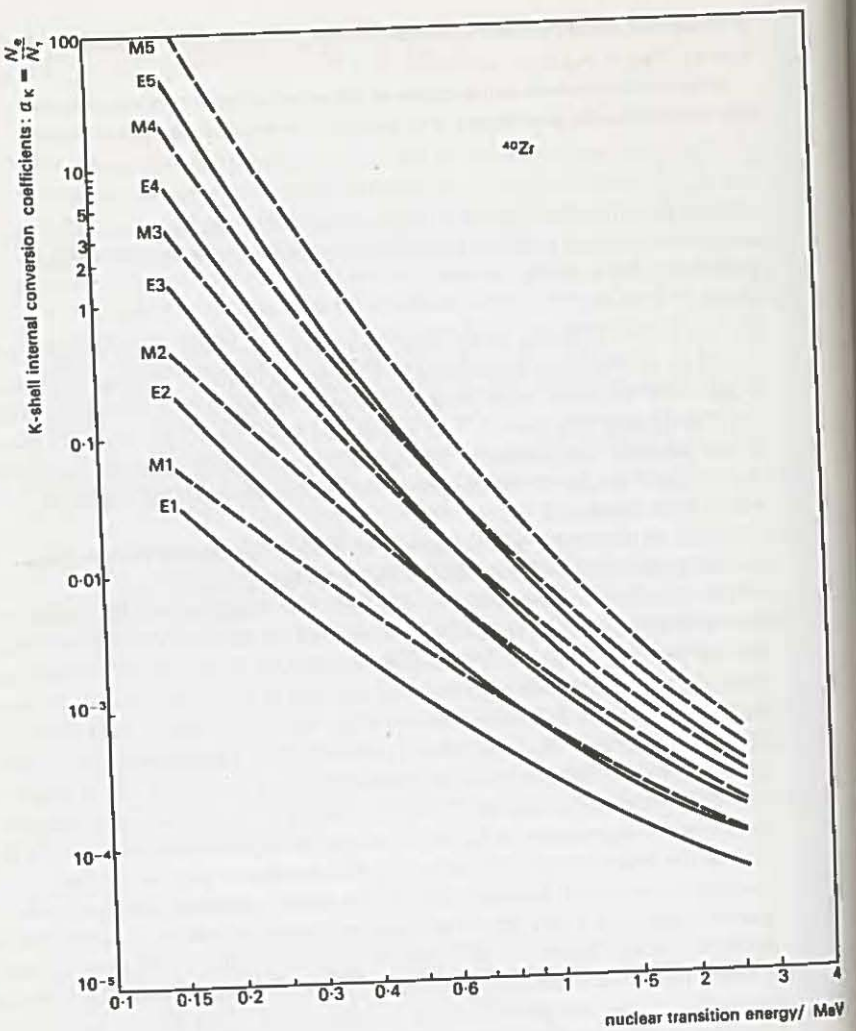

Figure 71 K-shell internal conversion coefficients as a function of nuclear transition energy for zirconium ($Z = 40$)

In addition to providing valuable information about the character of radiative transitions, the studies of internal conversion are important in two other respects. Firstly, a measurement of the energy of the emitted electron, together with a knowledge of the electron binding energy, permits a measurement of the transition energy to be made. This is a useful alternative to the methods of γ-ray energy measurements based on photoelectron production in materials external to the source. Secondly, if the transition energy is otherwise known, a measurement of

the electron energy permits an accurate determination of the electron binding energy. This knowledge can then be used to determine the Z of the atom within which the transition took place. The necessary experimental accuracy is set by the fact that there is a difference of about 2·5 keV in the binding energy of K-electrons in heavy nuclei differing by one in the Z-value. The importance of this Z-determination lies in being able unambiguously to decide whether a γ-ray transition took place before or after an α- or β-decay.

Finally it is to be noted that, following internal conversion, the atom is left with a vacancy in one of the electron shells. There will therefore be the emission of an X-ray or an Auger electron. It is sometimes more convenient to detect the X-ray or Auger electron rather than the conversion electron, and this information can be used to determine N_e, due allowance being made for the X-ray fluorescence yield (i.e. the number of X-rays emitted per vacancy).

10.9 Internal pair production

According to the 'hole' theory of positrons, the excited nucleus is immersed in a sea of electrons occupying and completely filling states of negative energy which correspond to the negative square roots of $p^2c^2 + m_0^2c^4$. If the transition energy is equal to $2m_0c^2 = 1{\cdot}022$ MeV, then sufficient energy is available to raise an electron from the highest of the negative-energy states to the lowest state in the positive continuum given by the positive square roots of $p^2c^2 + m_0^2c^4$. Should this occur then a stationary electron together with a vacancy in the highest

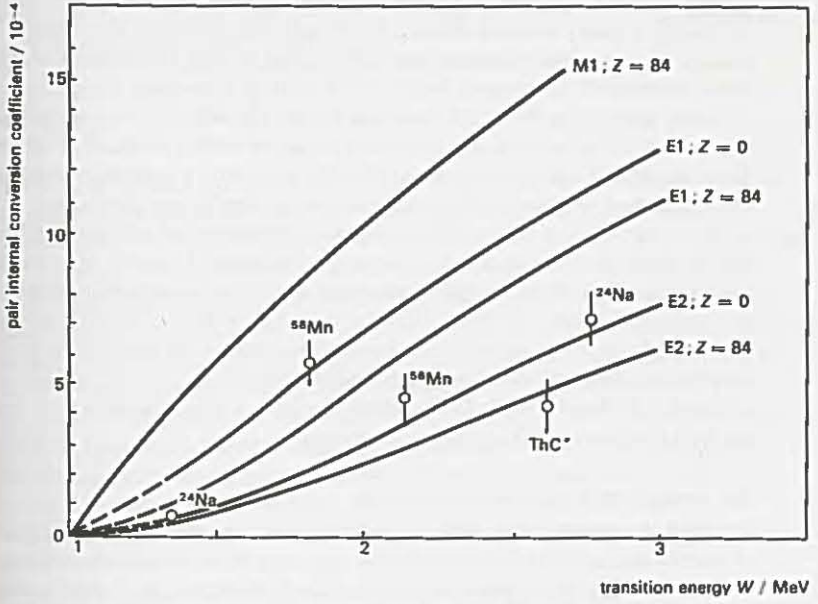

Figure 72 Internal pair conversion coefficients as a function of transition energy for nuclei of low and high Z-value

negative-energy state is produced. The vacancy constitutes a positron of zero kinetic energy. If the transition energy is greater than $2m_0c^2$ then an electron may be lifted from a lower-lying negative-energy state across the energy gap to a higher-lying state in the continuum. This constitutes the production of an electron–positron pair, the particles sharing the energy $E_0 - 2m_0c^2$. The availability of electrons to the nucleus does not, in this phenomenon, depend on Z. In fact the process is more likely, other things being equal, in light as compared to heavy nuclei. Also the likelihood of pair production increases with increasing transition energy. It is also favoured for low as compared to high multipole orders. In all these respects the probability of internal pair production behaves oppositely to that of internal conversion.

In Figure 72 the internal pair conversion coefficient, i.e. the ratio of pairs produced to photons emitted, is plotted as a function of energy for different multipolarities. The discrimination between multipole orders decreases with increasing transition energy. At higher energies, multipole orders can better be distinguished by the angular correlation between positron and electron, the angle between the particles being on average smaller the higher the multipole order.

10.10 $0 \rightarrow 0$ Transitions

We saw that $0 \rightarrow 0$ transitions cannot take place by the radiation of photons. While the field outside the nuclear volume is the same for both states, and therefore no electromagnetic field is generated in the transition, there can be a change in radius and a change in field within the nuclear volume. When there is no change in parity between the two states, internal conversion is a possible process. However, the transition rate will be small because the effective volume is small compared to the volume within which internal conversion can take place for other transitions. When the transition energy exceeds $2m_0c^2$, internal pair production is also possible, the pair being produced within the nuclear volume. There are several examples known of $0^+ \rightarrow 0^+$ transitions proceeding by internal conversion and others of similar transition proceeding by pair production.

In the case of $0^+ \rightarrow 0^-$ transitions, internal conversion and pair production, as well as single-photon radiative transitions, are forbidden. It would appear that the most likely mode of decay in such a case would be two-photon emission, or one-photon emission together with one conversion electron. Processes such as these are physically possible in the case of all transitions but have a very low probability compared to the processes discussed above.

There is no known excited state which, for lack of a possible decay mechanism, has an infinitely long life against de-excitation.

10.11 The measurement of energy-level spacing

We begin our consideration of the experimental measurements of the properties of excited states by surveying briefly the more important techniques which may be used for mapping out the energy levels. The problem is that of the accurate measurement of the energies of the emitted γ-rays. Many techniques are available for γ-ray energy measurements and we proceed to outline the most important of these.

10.11.1 *Curved-crystal spectrometer*

The use of a crystal lattice as a diffraction grating is well established in X-ray technology and provides an accurate way of determining the wavelength of the X-ray. For reflection from parallel planes of atoms which have a separation d, the Bragg angle at which reinforcement occurs is given by

$$\lambda = 2d \sin \theta,$$

where θ is the angle between the X-ray beam and the reflecting surface. The extent to which this technique can be extended in the direction of shorter wavelengths, i.e. higher quantum energies, is governed by the extent to which the crystal reflecting power falls off with increasing quantum energy and the extent to which the Bragg angle gets impractically small.

While the first of these effects has to be accepted, the second can be ameliorated by experimental ingenuity. To see the smallness of the Bragg angle involved in extending the technique to γ-ray measurements, let us consider the application of the method to the measurement of the wavelength of *annihilation radiation*. This radiation, which is emitted when positrons annihilate on electrons at rest, is a very convenient standard radiation with which to calibrate γ-ray spectrometers. When an electron of zero kinetic energy encounters a positron at rest it makes a transition down to the highest of the negative-energy states. Thus the energy of the gap, namely $2m_0c^2$, is available for radiation. However, in order that the final linear momentum of the system be zero, as was the initial linear momentum, two oppositely directed photons have to be emitted. Each photon therefore has an energy of m_0c^2, which is equal to 510·98 keV. The wavelength of this annihilation radiation is therefore

$$\lambda = \frac{hc}{m_0c^2} = 2{\cdot}43 \times 10^{-9} \text{ mm}.$$

For calcite, which has a lattice constant $d = 3{\cdot}02 \times 10^{-10}$ m, the Bragg angle for annihilation radiation is $\theta = 4 \times 10^{-3}$ rad. This means that a high degree of parallelism in the incident beam and a long distance of travel following reflection are necessary to separate the reinforced reflected beam from the incident beam. In most situations encountered in γ-ray spectroscopy the radiation is emerging from a small specimen so that the geometry called for using an orthodox crystal would impose a very low solid angle for acceptance of photons, and would lead to very low efficiencies. An ingenious method in which the crystal is curved enables the Bragg angle for photons sent through the crystal to be kept constant over a larger solid angle of emission from a point source (J. W. M. Du Mond, *Experimental Nuclear Physics*, Volume 3, Wiley, 1959) and makes it more practical to screen a γ-ray detector, set to detect reflected photons from the incident beam. With a curved crystal, the annihilation radiation spectrum, wavelength $2{\cdot}43 \times 10^{-12}$ m, has an instrumental full width at half-maximum of $0{\cdot}3 \times 10^{-13}$ m, i.e. about 1 per cent of the wavelength. The accuracy of determination of the position of the peak, i.e. the absolute wavelength, is believed

to be 0·04 per cent. Working under these conditions the overall detection efficiency is 5×10^{-8} counts per photon emitted from a point source.

10.11.2 *Magnetic spectrometers*

The γ-ray energy determination reduces to the measurement of the energy of an electron if advantage is taken of internal conversion or if the photons are allowed to interact with atomic electrons in a thin radiator and thus to produce photoelectrons, Compton electrons or electron-positron pairs (see Appendix C). The secondary electrons may then be sent into a uniform magnetic field H and their curvature ρ in the plane perpendicular to the field measured.

The electron momentum is then given by $30\,000 H\rho$, where H is in gauss, ρ in metres and the momentum in eV/c. Since the electron kinetic energy is comparable to its rest mass in these experiments, we must use the relativistic relation

$$E_e^2 = p^2c^2 + m_0^2 c^4$$

to find the total energy of the electron. The rest-mass energy $m_0 c^2$ may be subtracted from this to find the kinetic energy T_e. If the electron is an internal conversion electron or a photoelectron from the radiator, then we have simply to add the appropriate binding energy to T_e to arrive at the transition energy. If the electron is a Compton electron or an electron from a pair, then the energy T_e for a given value of H is no longer unique. A spectrum has to be measured and compared with theoretically predicted spectra for a range of γ-ray energies.

Energy resolution in a magnetic spectrometer can only be improved at the expense of reducing the solid angle of acceptance. A typical practical compromise, in which the electrons are bent round a semicircle from a radiator to a detector separated by a distance 2ρ, provides 1 per cent energy resolution at a photon energy of 1 MeV with an efficiency of 10^{-11} counts per photon.

10.11.3 *Proportional counters*

A proportional counter usually consists of a fine wire running coaxially along a sealed cylindrical metal tube and insulated from the tube. The wire is raised to a positive potential with respect to the tube. If any ionization takes place in the sealed volume of gas, the electrons produced are accelerated towards the wire. In the high field gradient in the neighbourhood of the wire an electron can gain enough energy between collisions to ionize the next gas molecule it encounters. In the resulting avalanche, the total charge collected by the wire can, with proper experimental design, be arranged to be proportional to the number of primary electrons produced by the ionizing particle.

The gas amplification produced in this way can amount to 10^3 without any loss of proportionality. The collected current is then passed through a high resistance and the resulting voltage pulse amplified to the height required to operate a pulse-height analyser. In the range of photon energies immediately

above the K-absorption edges of the gases used to fill the counter there is a high probability that a photon passed in through a thin window will be absorbed in the gas and produce a comparatively low-energy photoelectron, which will stop in volume of the counter. In this way the counter, with a choice of a gas of high atomic number, such as xenon, for a filling, can for photons of energies of 100 keV have a resolution of 3 per cent and an efficiency of 10 per cent.

In some cases the sample may be in gaseous form and suitable for introduction as a counter gas. Then, for low-energy transitions, K and L internal conversion electrons will stop in the gas; they are detected with 100 per cent efficiency and a very accurate measurement, not only of the transition energy but of the ratio α_K/α_L is possible.

10.11.4 *Scintillation spectrometers*

Charged particles produce not only ionization along their tracks but leave a trail of excited atoms which de-excite by radiating photons in the optical range of the electromagnetic spectrum. The light output from the particle track is proportional to the energy dissipated by the particle, which will be its total kinetic energy if the particle stops within the material. Certain crystals are quite transparent to this internally produced light. When this is so, the emergent light can be collected and passed to a photomultiplier, which will produce a charge proportional to the number of photons of light falling on its photocathode. This charge can be passed through a resistance and the voltage pulse amplified. Voltage pulses produced in this way and passed to a pulse-height analyser will then reproduce the energy spectrum of the charged particles.

A scintillating crystal, in addition to the necessary optical properties, requires to have a proportion of heavy nuclei incorporated in it if it is to efficiently convert incident photons into secondary electrons and stop them within its own volume. This condition is admirably satisfied by sodium iodide, which has found a very wide application in γ-ray spectroscopy. The crystal may be several centimetres in linear dimension and large enough to be operated under conditions approaching total absorption of the incident photon. In this case, (a) when photoelectric absorption takes place, not only is the photoelectron stopped in the crystal but the subsequently emitted X-ray is also absorbed; (b) when Compton scattering takes place, not only is the scattered electron stopped but the degraded γ-ray is absorbed and; (c) when pair production takes place, not only are both particles stopped but the annihilation quanta are also absorbed in the crystal. The crystal light output is then proportional to the total energy of the photon and a single peak in the pulse distribution is observed for a single γ-ray energy. In most cases, however, all the secondary photons are not absorbed and subsidiary peaks, *photon escape peaks*, are observed in the spectrum.

In the event of the source emitting two γ-rays from a cascade within a time short compared to the resolving time of the crystal and the associated electronic apparatus (say 10^{-6} s) then it is possible for both γ-rays to produce light pulses

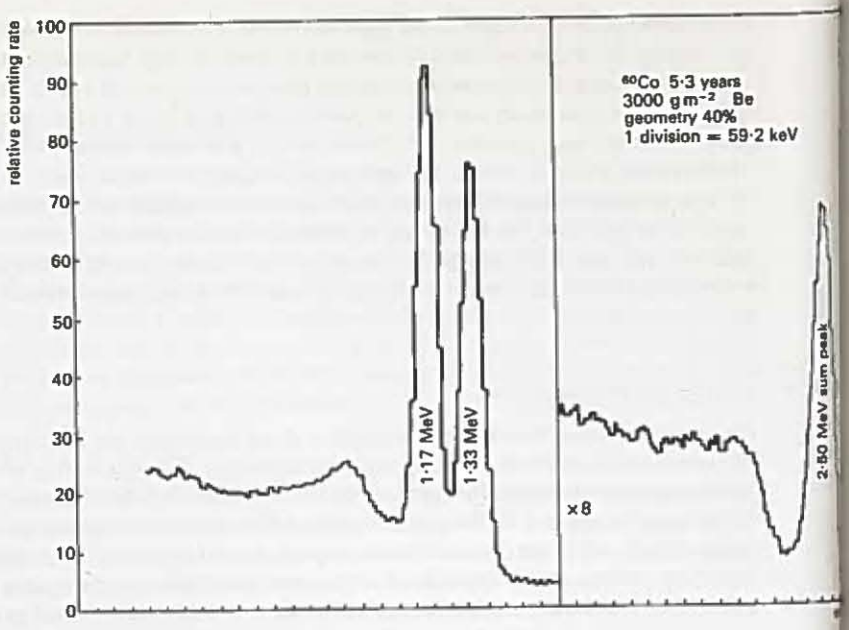

Figure 73 Energy spectrum of ^{60}Co measured with 10 cm x 10 cm NaI(Tl) crystal showing total energy peaks for the γ-ray lines at 1·17 MeV and 1·33 MeV together with the sum peak. The γ-rays were passed through a beryllium filter

which add together at the photocathode of the multiplier. There is thus the possibility of a *sum peak* in the spectrum. An indication of the attainable performance from a 10 cm x 10 cm cylindrical sodium iodide (thallium activated) crystal is given in Figure 73. The counts per emitted photon from a source can exceed 0·1 and, as is seen from the figure, the energy resolution is about 8 per cent. The energy resolution depends both on the statistical fluctuations in light emitted as a function of energy dissipated and in the variation of efficiency of light collection from different regions of the crystal.

Scintillation counters offer very high efficiencies compared to magnetic spectrometers or curved-crystal spectrometers but their resolution is considerably inferior.

10.11.5 *Solid-state detectors*

The advent of solid-state detectors has enabled γ-spectroscopy to proceed with the high resolution of magnetic spectrometers and with an efficiency approaching that of heavy scintillators. This, as we shall see, has had very important consequences in experimental nuclear physics.

The physical principle involved in solid-state detectors concerns electrical conductivity in a crystal. In the case of a perfect crystal, all the electrons are in the filled band which lies, with a band gap of about one electronvolt, below the conduction band. If two electrodes are connected to opposite faces of the crystal and a voltage difference maintained between them, there will be no flow of current. However, a charged particle passing through the crystal can promote the electrons from the filled to the conduction band. There is a consequent flow of current. The energy necessary to promote an electron and thus produce an electron–'hole' pair is on the average about three electronvolts, which is to be compared with thirty electronvolts necessary to produce an ion pair in a gas. The movement of the electron and the 'hole' through the crystal is very fast compared with the movement of electrons and positive ions in a gas counter. It is therefore to be expected, because of the larger number N of electron-hole pairs produced compared to ion pairs for a given energy dissipated, that the statistical variation, which will be proportional to $1/\sqrt{N}$ will be smaller and that this will lead to better energy resolution. At the same time, because of the high mobility of the electrons and holes, the counter can have a very fast response time.

The achievement of a practical detector based on this principle is not however a simple matter. In a real as distinct from an ideal crystal, the conduction band is never in fact completely unoccupied. Electrons are raised into it by thermal fluctuations and, usually more importantly, by the action of impurity centres in the crystal. In the semiconductors silicon and germanium, it has proved possible by 'doping' (i.e. by introducing impurities in a controlled way) to compensate for the unavoidable natural imperfection of the crystal and so to approach the behaviour of an ideal crystal. This has been achieved by drifting lithium ions moving under the influence of an applied electric field into a pure silicon or germanium crystal. Germanium has a special interest for γ-ray spectroscopy because of its high atomic number. In practice there is the complication that the crystal has to be used and stored at liquid-nitrogen temperature, otherwise its performance is seriously impaired by lithium diffusing out.

Germanium crystals with a sensitive volume of a hundred cubic centimetres are now commercially available. Their efficiency is such that the number of counts in the total absorption peak of the spectrum can be 2–3 per cent of the number of γ-rays falling on the detector for γ-rays of two million electronvolts energy. The efficiency rises to much higher values at lower energies but falls off quite rapidly at higher energies. The intrinsic time resolution of the detector can be less than 10^{-8} s.

A spectrum of ^{60}Co measured with a 40 cm^3 lithium drifted germanium detector is shown in Figure 74. Comparison of this spectrum with the sodium iodide spectrum in Figure 73 gives a clear indication of the improvement effected by the development of solid-state detectors. With their help it is now possible, even when only comparatively weak sources are available, to measure level spacing to five significant figures.